OCTOBER 1975 MATT-1160

PARAMETRIC INSTABILITIES AND PLASMA HEATING IN AN INHOMOGENEOUS PLASMA

BY

M. PORKOLAB, V. ARUNASALAM,
N. C. LUHMANN JR., AND
J. P. M. SCHMITT

PLASMA PHYSICS LABORATORY

PRINCETON UNIVERSITY
PRINCETON, NEW JERSEY

This work was supported by U. S. Energy Research and Development Administration Contract E(11-1)-3073. Reproduction, translation, publication, use and disposal, in whole or in part, by or for the United States Government is permitted.

DISCLAIMER

NOTICE

Printed in the United States of America.

Available from
National Technical Information Service
U. S. Department of Commerce
5285 Port Royal Road
Springfield, Virginia 22151
Price: Printed Copy $ *; Microfiche $1.45

*Pages	NTIS Selling Price
1-50	$ 4.00
51-150	5.45
151-325	7.60
326-500	10.60
501-1000	13.60

PARAMETRIC INSTABILITIES AND PLASMA HEATING IN AN INHOMOGENEOUS PLASMA.*

M. PORKOLAB, V. ARUNASALAM, N. C. LUHMANN JR.,† and J. P. M. SCHMITT‡.
Plasma Physics Laboratory, Princeton University
Princeton, New Jersey 08540 USA

ABSTRACT

Experimental studies of plasma heating due to microwave irradiation of the magnetically confined plasma column in the Princeton L-3 device is presented. X-band (10.4 GHz) microwave power, both in the ordinary and the extraordinary modes of propagation, is used in these experiments. Plasma heating is observed to occur simultaneously with the occurance of parametric decay instabilities. The mode structure of the pump wave and the decay ion wave dispersion has been measured with high frequency probes. Detailed measurements of electron heating rates are presented and compared with collisional heating rates. In addition, production of suprathermal electrons and ions is also observed and measured. A comparison is made with recent laser-pellet interaction experiments.

---

† Present address: Department of Electrical Sciences, University of California, Los Angeles, California.

‡ Present address: Laboratoire de Physique des Milieux Ionises, Ecole Polytechnique, Palaiseau, France.

I. INTRODUCTION

Because of possible applications to laser pellet interaction and rf heating of magnetically confined plasmas, the study of parametric instabilities and associated plasma heating is of considerable importance[1,2].To present date most experimental studies of parametric instabilities and plasma heating have been performed in uniform plasmas. However, it has been shown in a number of theoretical papers that inhomogeneities of density, temperature, or magnetic field may considerably modify the nature of these instabilities, and consequently the associated plasma heating[3].Therefore it is of interest to perform experiments in inhomogeneous plasmas to test the validity of these theories, and to determine what type of plasma heating one may obtain. This requires either sufficiently high temperatures and/or sufficiently collisionless plasmas, and electromagnetic waves incident onto an inhomogeneous plasma from the outside. In order to study some of these effects, we set up an experiment in the Princeton L-3 device where a fast rise time (50 nano-sec) X-band (f_o = 10.4 GHz, λ_o = 2.9 cm) collimated microwave beam (approximately 3.5 × 3.5 cm illumination area) was radiated onto the magnetically confined plasma column. Depending upon the polarization of the incident electric field two modes of operation were used: (a) The ordinary ("O") mode of propagation ($\vec{E}_o \| \vec{B}$ where $\vec{B}$ is the external dc magnetic field); (b) The extra-ordinary mode of propagation ("EO", where $\vec{E}_o \perp \vec{B}$). In the O mode of propagation decay into electron plasma waves (Bohm and Gross or Langmuir waves) and ion acoustic waves is expected to occur[2,4].In the case of

EO mode decay into upper hybrid (Bernstein) and lower hybrid or ion acoustic waves is expected to occur[2,5].In particular, since in the present experiments $\omega_{pe} \gtrsim 2\Omega_e$, $\omega_{pi} \simeq 100\Omega_i$, we have for the most unstable mode, $\omega \simeq \omega_{pi}/4$, $\omega_{ci} << \omega$ (where $\omega_{pe}(\omega_{pi})$ is the electron (ion) plasma frequency, and $\Omega_e(\Omega_i)$ is the electron (ion) cyclotron frequency). The plasma diameter has been varied between 5 and 10 cm so that $\lambda_o < d$. The density gradient scale length is typically $H \simeq 1$ to 3 cm, so that $\lambda_o \simeq H$, and the most unstable wavelength is of the order of $\lambda = 0.1$ cm so that $\lambda/H << 1$. Under these conditions we expect that in the ordinary mode of propagation the magnetic field effects can be ignored, and that for a large range of acoustic frequencies and wave-numbers (i.e., $\omega_{ci} < \omega$) the WKB approximation should hold when density gradient effects are included in the growth rate calculations[3].On the other hand, WKB type of solutions for the incident wave will not be valid. Nevertheless, the present scaling, (i.e., sharp gradients) is very similar to recent results obtained in laser-pellet interactions(as well as in RF heating of fusion plasmas near the lower-hybrid frequency) and hence it is of great interest to study this regime[6,2].

There have been only a few experimental studies of plasma heating due to parametric instabilities near the $\omega \simeq \omega_{pe}$ layer, especially in inhomogeneous plasmas (which is the case of interest in laser fusion). In particular, Dreicer et al. reported observation of suprathermal electrons produced during studies of anomalous absorption by rf cavity techniques[7]. In this Q-machine experiment $T_e \simeq T_i$, and collisional losses are sufficiently high so that the homogeneous theories apply. (In

addition, the main heating was observed in the uniform region of the plasma). More recently Mizuno and Degroot reported observation of parametric instabilities and plasma heating in a plasma filled waveguide system[8].In this case mainly studies on energetic tail formation were made. The most similar experimental arrangement to ours are those of Eubank [9] and Okabayashi et al. [10]. Both of these experiments were of preliminary nature, and thus: (a) no detailed measurements of the decay waves were made; (b) due to the slow rise time of the microwave system (milliseconds) no detailed measurements of the initial heating rates could be made. Because of the slow rise times, ionization problems were also present. In addition, no focusing device (horn) was used to collimate the incident microwave beam. We had rectified these problems in the present experiment, and obtained further experimental data on the details of plasma heating associated with parametric instabilities. Preliminary results of this work had been presented at a recent conference [11]. The plan of the paper is as follows: In Section II we summarize the results of inhomogeneous plasma theory, in Sections III and IV we present the experimental results on the O^0 and EO mode of propagation, and in Section V the Summary and Conclusions are given.

II. SUMMARY OF THEORY

In an inhomogeneous plasma the thresholds and growth rates of parametric decay instabilities may change due to convective losses. As shown by Perkins and Flick, [3] the instabilities may become convective, and for the parametric decay the following

effective threshold (i.e., a total amplification of exp(A) is obtained) has been obtained for the O mode:

$$\frac{E^2}{4\pi n_o T_e} > \frac{1.6A}{k_{\parallel} H}\left(\frac{\nu_i}{\omega_1}\right)^{1/2} + 4\left(\frac{\nu_i \nu_e}{\omega_1 \omega_o}\right) \qquad 1(a)$$

for strongly damped waves, and

$$\frac{E^2}{4\pi n_o T_e} > \frac{2.4A}{k_{\parallel} H}\left(\frac{k_{\perp}}{k_{\parallel}}\right) + 4\left(\frac{\nu_i \nu_e}{\omega_1 \omega_o}\right) \qquad 1(b)$$

for weakly damped waves [i.e., for $k_{\perp} c_s > (\omega_1 \nu_i)^{1/2}$]. For $T_i << T_e$, we have the following definitions:

$$\frac{\nu_i}{\omega_1} = \left(\frac{\pi m_e}{2m_i}\right)^{1/2} + \frac{\nu_{io}}{2\omega_1} \; ; \quad \omega_1 = k c_s \quad , \qquad (2)$$

where ν_i is the damping rate of the ion acoustic wave, ω_1 is its frequency, $k^2 = k_{\parallel}^2 + k_{\perp}^2$, $k_{\perp} < k_{\parallel}$, $c_s = (T_e/m_i)^{1/2}$ is the acoustic speed, ν_{io} is the ion-neutral collision frequency, T_e is the electron temperature (measured in units of energy), n_o is the equilibrium density, H is the density gradient scale length, and A is the number of e-folding the decay waves are amplified as a function of pump power. We note that an approximate lower limit on $k_{\perp}$ can be obtained from the condition of violation of the WKB approximation, i.e., $k_{\perp} \sim 1/x$. Using the Langmuir wave dispersion relation

$$\omega^2 = \omega_{pe}^2\left(1 + \frac{x}{H}\right) + 3\,(k_{\perp}^2 + k_{\parallel}^2) v_{te}^2 \qquad (3)$$

we obtain

$$k_{\perp min} \simeq \frac{1}{H^{1/3}\lambda_D^{2/3}} \quad , \tag{4}$$

where $\lambda_D = v_{te}/\omega_{pe}$ is the electron Debye length, and $v_{te} = (T_e/m_e)^{1/2}$ is the electron thermal speed. Thus, we see from Eq. 1(a) and 1(b) that the threshold increases with decreasing values of $k_{\parallel}$ (i.e., frequencies) for both weakly and strongly damped ion acoustic waves. The reason for this is that the amplification rate decreases with longer wavelengths since the convective losses increase. We note that this result is valid only for the O-mode of propagation, and that similar calculations in inhomogeneous plasmas for the EO mode are not available. Therefore, we shall compare our results of the EO mode with theories of homogeneous plasmas [5]. Note that in Eqs. 1(a), 1(b) in the right hand side the last term corresponds to the results of uniform plasma theory [3,4]. Thus, in order to be in the regime of inhomogeneous plasma theory we need in the right hand side the first term (i.e., the term proportional to $1/(k_{\parallel}H)$) dominate the second term. This requires sufficiently small values of (ν_e/ω_o). If the inhomogeneous term dominates, the spatial growth rate is given by [3]

$$E^2(x) = E_o^2 \exp(A)$$

where A is given by Eqs. 1(a) and 1(b). In the published literature [3] for growth of fluctuations from background noise an "effective threshold" of $A = 5$ (or 2π) was chosen arbitrarily.

In the present work for threshold we shall use $A = 1$ (since we can monitor the initial fluctuation level).

III. EXPERIMENTAL RESULTS FOR THE ORDINARY MODE OF PROPAGATION

The experimental set up is shown in Fig. 1. The plasma is produced by a slow wave structure fed by a 1 kW S-band (2.45 GHz) microwave source which operates in the non-resonant ($\omega_o < \Omega_e$) mode [12]. Typical plasma parameters are as follows: $n_{max} \lesssim 3 \times 10^{12}$ cm^{-3}, $T_e \simeq 5$ eV, $T_i \simeq 0.1$ eV, $B_o \simeq 2$ kG, $P \simeq 2 \times 10^{-3}$ Torr in Helium gas, and $n_{crit} = 1.35 \times 10^{12}$ cm^{-3} (where n_{crit} is defined as $f_o = f_{pe}(n_{crit})$). A 3.5 kG mirror can be energized at the ends of the 1.6 m long uniform ($\Delta B/B < \pm 0.15\%$) device. The fast rise-time ($\tau \simeq 50$ nanosec) X-band microwave power is radiated via a focusing horn onto the plasma column approximately near the center of the device (1 m from the slow wave structure). In vacuum the horn collimates the microwave beam up to the center of the chamber into a cross-sectional area of 3.5×3.5 cm. However, with the plasma present some refraction of the microwave beam is observed, and high frequency fields within the width of the horn in a cylindrical shell around the plasma column are observed. We believe that similar effects may also occur in laser-pellet interaction, in which case an even more complicated spherical shell of electromagnetic radiation could form around the pellet. Therefore, as we shall see, it is rather difficult to calculate the local electric fields near the critical surface. Typical diagnostics include an electrostatic multigrid energy analyzer, Langmuir probes, a fast rise time diamagnetic loop, axially and radially moveable high frequency

probes, X-band receiver and spectrum analyzer, and an 8 mm microwave interferometer for measuring density. In Fig. 2 we show measurements of a typical density gradient (as determined by a Langmuir probe), and for obtaining the proper perspective we superimposed a schematic sketch of the X-band free-space wavelength. This shows that the average diameter of our plasma column corresponds to three to five free-space X-band wavelengths (not unlike CO_2 laser wavelength-pellet size ratios). In actual measurements the X-band waves were found to be partially standing waves due to reflections from the plasma column.

As the incident power was raised above 15 watts, (i.e., $E_o/(4\pi n_o T_e)^{1/2} = v_D/v_{te} \simeq 10^{-2}$) parametric decay spectra with maximum amplitudes near 25 - 30 MHz ($\sim f_{pi}/4$) was picked up by high frequency probes immersed in the plasma near the critical layer. The low frequency ion wave spectrum and the high frequency sidebands about the pump frequency satisfied the usual frequency selection rules, $\omega_o = \omega_1 + \omega_2$. Typical decay spectra considerably above "threshold" is shown in Fig. 3(a). Note that at intermediate power levels (237 watts) the spectrum extends to f_{pi} (112 MHz), the ion plasma frequency. However, at very high powers the spectrum extends even somewhat above f_{pi}. Also, at very high powers the spectrum piles up in the very low frequency components, unlike at intermediate or low power levels.

We have attempted to measure effective "thresholds" or growth rates as predicted by Eq. 1(a), 1(b). In Fig. 3(b) we show an example of effective threshold (which we defined at A = 1 in Eq. 1) as a function of ω(i.e., k). The functional variation indicates good agreement with Eq. 1. In particular, this figure

shows that the threshold decreases with increasing frequencies (wave-numbers) up to about $f_{pi}/4$, and then increases. However, note that the higher frequency components ($f > f_{pi}/4$) are present, even though linear theory would predict stability due to strong Landau damping at the corresponding sidebands. Although these higher frequency modes are clearly present, their amplitudes (and also the amplification rates which we measured later) are smaller than those of the most unstable modes. It is possible that the higher frequency components are generated by nonlinear effects. The threshold of the most unstable wave ($f \simeq 25$ MHz) is in good agreement with the inhomogeneous threshold at $A = 1$, i.e., $P_{th} = 16$ W, $v_D/v_{te} \simeq 10^{-2}$, and it is approximately an order of magnitude (in power) above the homogeneous threshold ($P_{th} \simeq 1.6$ W, $v_D/v_{te} \simeq 3 \times 10^{-3}$).

We have made further experiments by using different diameter plasma sources, and operated under various conditions, so as to generate different types of density profiles. The gradient scale-lengths were varied from $H = 1$ to 3 cm, and the density profiles were not always exponential as in Fig. 2. In contrast to the results shown in Fig. 3(b) we found that the threshold curves were not a "typical" result, but rather a special case. In general, the inhomogeneous threshold theory (Eq. 1) was not always obeyed; rather, the amplification rates were often independent of wave number (or frequency) even for $f < f_{pi}/4$. An example of such a case is illustrated by Fig. 4, where we show amplification of individual wave packets which were selected by appropriate filtering and heterodyne techniques. We note that in this case the amplification as a function of pump power is nearly independent

of wave number, and that the only clear tendency is a definite reduction in amplification rates above $f \simeq f_{pi}/4$ (or 25 MHz) (a sign of Landau damping). These results are in clear contrast to the predictions of inhomogeneous plasma theory, i.e., Eq. 1.

The radial location of decay wave amplitude and relative pump wave level is shown in Fig. 5. In Fig. 5(a) we show that the incident power is strongly decreasing before the critical layer, and that it refracts around the plasma column (which in the present case had a bell shaped profile with its center located near $r \simeq 1$ cm). Note that the decay spectrum is peaked near $r \simeq 2.5$ cm, just outside the critical layer (which was approximately $r \simeq 2.2$ cm), and that a smaller peak is present on the opposite side of the plasma column due to the refracted (and in general lower amplitude) microwave beam. From this picture we see that the decay instability is located in a strongly nonuniform rf pump field, with its amplitudes decreasing at scale lengths comparable to the gradient scale length of increasing plasma density. This is in contrast to the usual theories which assume a constant pump field [3]. Furthermore, the actual local pump electric fields near the critical surface are smaller than one would obtain from calculations using the incident pump power and vacuum field radiation patterns. Because of complications arising from refraction effects, and technical difficulties arising when we tried to measure the local electric fields with probes, we were unable to determine quantitatively the local pump electric fields. Hence, in this paper we shall quote the vacuum electric fields calculated from the radiation pattern of the horn. According to Fig. 5(a) the actual local electric

fields near the critical layer could be smaller than the incident electric fields by a factor of 3 to 5, and thus the observed thresholds are well within an order of magnitude of uniform plasma theory. Because of the presence of the magnetic field, we do not believe that linear mode conversion is of importance in the present geometry. Our attempts to detect such linearly converted waves proved negative.

In order to verify that the low frequency decay waves were ion acoustic waves, we carried out interferometric measurements somewhat above threshold using band-pass filters. In such a manner the dispersion relation for ion acoustic waves with frequencies up to 15 MHz (or $\lambda_{\parallel} \simeq 0.75$ mm) were verified. Figure 6 shows the results of such measurements. We also show a typical interferometer output of an ion acoustic wave packet at f = 7.5 MHz, near the center of the microwave horn. Similar data was used to obtain the dispersion curve of Fig. 6. Higher frequencies could not be measured with the present probe techniques since the wavelengths became comparable with probe dimensions. Also, for higher pump powers ($P_{in} > 400$ W) the cross correlation distances became comparable with wavelengths, indicating transition to strongly turbulent regimes.

In addition to studying the mechanism of parametric decay, the important goal in our experiment was to study anomalous heating of the plasma. This requires a fast rise-time microwave pulse so that heating rates faster than the classical collisional value could be detected. In our plasma the total electron-ion and electron-neutral collision frequency is $\nu_i \simeq 6 \times 10^6 \text{sec}^{-1}$. The rise time of the microwave system was $\tau \simeq 50$ nsec, which proved to be

sufficiently short to demonstrate the presence of anomalously fast main body plasma heating. In Fig. 7 we show results of the retarding potential electron energy analyzer measurements of the electron distribution function at low and at high rf pump powers. We see that at low power (P_{in} = 118 W) the temperature increased from $T_e \simeq 5$ eV to about 6.5 eV. There was also a small energetic tail present (not shown here). At higher power level a larger tail as well as more main body heating was observed. The distribution function is of a two-component Manwellian form. These results were obtained for microwave pulses of a few microseconds in duration. Once the pulse length was increased over τ = 3-4 μsec, the heating remained independent of time. The growth rates are sufficiently large so that in one microsecond the parametric decay spectrum was fully developed and saturated. Of course, at high pump powers the purely growing mode [4] could also be excited. However, the detection of this mode is difficult, and we have not made detailed measurements concerning the presence or absence of such an instability in the present experiments. From these and similar measurements we find that at the highest power levels used ($P_{in} \sim 4$ kW) at most a few percent of the particles were in the tail. The temperature of the tail was $T_e \lesssim 50$ eV for main body temperatures of the order $T_e \lesssim 20$ eV. Also, even at the maximum input power of $P \simeq 4$ kW (i.e., $v_D/v_{th} \simeq 0.2$) the observed maximum particle energies were limited to $\varepsilon \lesssim 0.5$ keV. We note that these results compare qualitatively with the predictions of the nonlinear theory and computer results for the case of finite interaction region of Thompson et al. [13]. Of

course, the detailed nature of suprathermal tail formation (such as number of particles and maximum particle energies) depends crucially on the size of interaction region and hence no quantitative agreement between real and computer experiments could be expected.

In Fig. 8 we show energy analyzer measurements of energetic ions. It can be seen that for input powers of 1.4 kW ions with energies up to 30 volt are present, and that the ions are drifting with a mean energy of $\varepsilon \simeq 15$ volt. Such drifting ions were present for input powers above threshold (10 W), and with increasing input powers a significant increase in ion energies was observed. At maximum input powers of $P_{in} \simeq 5$ kW($v_D/v_T \simeq 0.2$) ions with maximum energies of 60 volt were detected, which corresponds approximately to the mean energy (temperature) of the suprathermal electrons. Maximum drift velocities were approximately 15-20 volt, and the number of particles in this tail were approximately equal to the number of electrons in the electron tail (i.e., ~ 1-2%). We remark that since the transmission coefficient of ions passing into the energy analyzer are not known accurately, the accuracy of estimating the number of ions in the tail is not very good (order of magnitude estimate). We have also made spectroscopic measurements of main body heating of ions (initially $T_i \lesssim 0.1$ eV). However, we could not detect significant main body ion heating during the short pulses ($\tau < 10$ μsec). Finally, we note that radial scans with the energy analyzer showed that both electron and ion heating were localized to regions where the parametric decay waves had large amplitudes (near the critical layer) and had the same radial distribution as that shown in Fig. 5(b).

We have also performed measurements of heating with a shielded diamagnetic loop. Figure 9 shows the results of such measurements. We see that some heating occurs above threshold (10 W), and that considerably higher rate of heating occurs above P_{in} = 100 W. These measurements tend to corroborate the retarting potential energy analyzer measurements (i.e., that significant heating occurs only above threshold for parametric instabilities). The total perpendicular energy increase at P_{in} = 4 kW corresponds to approximately $\Delta T_{\perp} \simeq 2$ eV, as determined by the calibrated diamagnetic loop. We note that this is approximately an order of magnitude less than the parallel heating, $\Delta T_{\parallel}$.

Since a considerable fraction of the energy (in some cases most of the energy) went into main electron body heating, we performed measurements of the main temperature near the peak of the parametric instability region (which also coincided with the location of the peak temperature) as a function of time and input power. These measurements were done by a Langmuir probe and box-car integrator sampling technique. The probes were located downstream from the microwave region so that spurious rf pickup problems would not occur. (The energy analyzer was removed during these measurements). Figure 10(a) shows the results of such measurements. We see that similar to the energy analyzer measurements, beyond a few microseconds the heating saturates. In addition, as the input power (and hence heating rate) is increased, the saturation occurs at somewhat earlier times. This suggests that in the present experiment convective losses out of the region of heating may considerably limit the maximum electron temperature. Similar saturation

effects have been observed by Grek during studies of parametric heating near the cyclotron harmonic frequencies [14]. In Fig. 10(b) we plotted the average rate of change of temperature in the first few microseconds. We see that the heating rate increases roughly linearly with input power. At low powers (P_{in} < 100 W) the heating could be increasing faster than linearly with input power. However, due to background fluctuations and small changes in temperature in this regime we could not make quantitative measurements. At high powers (P_{in} > 1 kW) the heating rates saturate. This may be due to increased losses, and/or saturation of the response time of our diagnostic system (the latter is not reliable for times less than one μsec). A quantitative comparison of the slope of Fig. 10(b) indicates heating rates a factor of 20 faster than classical collisional absorption (due to coulomb and electron-neutral collisions). Thus, we conclude that for input powers a factor of five or more above threshold the main body electron temperature is heated anomalously fast due to the simultaneously occuring (and localized in the same radial position) parametric instabilities.

Finally, we should mention that we have also attempted to measure the possible presence of anomalous reflection and/or absorption directly, using directional couplers in the waveguide (placed just before the incident microwave horn). However, these measurements showed only 7% reflection, almost independent of incident power. We concluded that most of the incident power was absorbed and/or convected away by refraction around the plasma column, and thus the receiving cross section of the transmitting horn (which was located approximately 5 cm from the

plasma column) was too small to make meaningful measurements.

IV. EXTRAORDINARY MODE OF PROPAGATION

We have also performed heating experiments in the extraordinary mode of propagation. In Fig. 11(a) we show the amplitudes of the decay spectrum at three different power levels and in Fig. 11(b) we show typical thresholds for parametric decay. The decay layer in the present case was near the electron plasma frequency, (since at $f_o \simeq f_{UH} = 10.4$ GHz, $f_{ce} \simeq 4.5$ GHz, f_{pe}(crit.) $\simeq 9.5$ GHz). We note that since $H \gtrsim \lambda_o$, there is sufficient tunneling for the incident waves to get to the upper hybrid layer. The most unstable wave is near $f \simeq 50$ MHz, which is slightly above the local lower hybrid frequency ($f_{LH} \simeq 45$ MHz near the critical layer for f_{UH}). As the pump power is increased we see from the spectrum that ion acoustic waves ($f < 40$ MHz) as well as some cold lower hybrid waves (Trivelpiece-Gould modes) ($f > 60$ MHz) are excited. The spectrum around the pump frequency showed the presence of a lower sideband, which was the image of the low frequency spectrum. Because of the expected very short wavelengths, interferometric techniques with probes did not work in the present experiments. However, earlier measurements by Grek and Porkolab in a uniform plasma in a capacitor geometry corroborate such assumptions [14]. We also note that similar spectra was also observed in the FM-1 spherator at Princeton [10] in the regime $\omega_{pe} << \Omega_e$.

In Fig. 12 we show the electron distribution function due to the parametric decay. We see that both main body and tail heating occurs, and that the results are quite similar to those

obtained in the ordinary mode of propagation. Again, a few percent of the particles (up to 5%) were in the tail at $P_{in} \simeq 4$ kW, and particle energies above 0.5 kV were not observed. Measurements of electron temperature with Langmuir probes were also similar to those obtained in the O-mode, with typical heating times of one to two microseconds. Heating of the ion tail has also been observed, with a typical mean drift energy of 15 eV, and a broadening of 4 eV for input powers of $P_{in} \simeq 2$ kW and pulse length of 10 μsec. For longer pulse lengths ionization took place, and no measurements were taken.

In Fig. 13 we show a summary of the localization of heating in the EO mode, and parametric decay in a plasma with rather steep density gradients. Note the effects of refraction of the electromagnetic wave around the plasma column (i.e., decay on both sides), as well as the localization of the decay waves and ion heating. These both strongly suggest that ion heating is associated with the presence of the low frequency fluctuations and possibly acceleration by the expanding suprathermal electrons (also localized in the same layer.) The sideband upper-hybrid (or Bernstein) waves were also localized in this same layer, as well as the observed electron heating, as shown in Fig. 14. Note that the instability (and heating) regions are localized in regions of strongly decreasing electric fields and density gradients, hence a quantitative comparison of thresholds and growth rates with theories assuming constant rf pump fields is not justified. However, it is interesting to note that similarly to the O-mode and to the FM-1 experiments [10], the estimated local threshold fields near the critical layer were not too different (i.e., well

within an order of magnitude) of the predictions of uniform plasma and rf field theories [5]. Of course, the incident power is higher since tunneling must take place. Since much of the results obtained in the present experiments ($\omega_{pe} > \Omega_e$) at high powers in the EO mode of operation were quite similar to those of the O-mode, we shall not present any further data here.

V. SUMMARY AND CONCLUSIONS

We have studied excitation of parametric instabilities during microwave heating of a magnetized plasma. Since the magnetic field was weak (i.e., $\Omega_e < \omega_{pe}$) the heating observed during both ordinary and extraordinary mode of irradiation was quite similar. For the ordinary mode of excitation the decay waves have been measured, and the waves were identified to be ion acoustic waves. The waves were localized in a narrow packet in the density gradient, in the vicinity of the critical layer, and at high powers had frequencies from $f \simeq 0$ to f_{pi}. The lower sideband was believed to be Langmuir waves (from frequency and wave-number matching.) The threshold for instability of the different wave-number components depended on the background plasma conditions, and followed the predictions of inhomogeneous plasma theory only occasionally. In particular, a number of different density profiles were tried but in all cases $H = (\nabla n_o/n_o)^{-1} \gtrsim \lambda_o$, and in many cases the threshold for decay was nearly independent of the wave number (frequency) of decay waves. There could be several reasons for the irreproducibility of non-uniform plasma theory. (a) Refraction of the incident microwave beam around the plasma column was always observed; (b) The pump

electric fields were inhomogeneous (i.e., strongly decreasing in front of the critical layer) where the parametric decay instability was localized (i.e., $(\nabla n_o/n_o)^{-1} \simeq \lambda_o \simeq \nabla|E_o|/|E_o|$). (c) The density gradients were not always linear (as usually assumed by parametric theories). (d) The initial background fluctuation level was often as high as $\tilde{n}/n_o \simeq 5\%$. (e) Nonlinear interactions among the different wave-number components may be strong. Thus, we believe that some of these effects may be sufficient to invalidate the predictions of the usual theories of parametric instabilities in inhomogeneous plasma. The importance of some of these effects have been discussed recently [15].

The important conclusion obtained in the present work is that even in the presence of sharp density gradient $[(\nabla n_o/n_o)^{-1} \simeq \lambda_o]$ strong parametric decay instability was observed near the critical layer. The local threshold (near the critical layer) for these instabilities was comparable with the predictions of uniform plasma theory (well within an order of magnitude) in both the ordinary and the extraordinary modes of propagation. However, this corresponded to approximately an order of magnitude higher incident power levels (possibly due to tunneling and refraction effects.) Measurements of plasma heating showed the formation of two-component Maxwellian distribution function of electrons with a few percent of the particles in the tail for input powers 3 orders of magnitude above uniform plasma thresholds. However, the maximum tail temperatures were within a factor of five of the main body temperature (cold component), and the maximum particle energies observed were at most only a factor of fifty higher than the mean energy of the cold component. Direct

measurements of the heating rate of the main body of electrons (cold component) showed an anomalously fast heating rate, namely a factor of twenty faster than classical collisional absorption. The heating was localized to regions where the strong parametric decay instability was present. We postulate that nonlinearly generated short wavelength components may be responsible for the fast heating of the main body [13] (in particular, strong decay spectrum was observed with frequencies up to the ion plasma frequency, i.e., $k\lambda_D \simeq 1$). Alternatively, other nonlinear effects, such as resonance broadening [16] may have to be invoked to explain the present results. A group of energetic ions was also observed, with maximum energies of the order of the mean energy of the suprathermal electrons.

A comparison of these results with laser-pellet interaction experiment [6] strongly suggest that the observed good laser absorption, the lack of extremely energetic suprathermal electrons, and the generation of energetic ions may be consistent with the excitation of the parametric decay instability near the critical layer. In particular, the presence of the magnetic field and strong gradients in our experiments shows that the presence of self-generated magnetic fields and strong density gradients observed in laser experiments [17] do not necessarily prevent the excitation of strong parametric decay instabilities. In particular,recently Grek et al [18] in CO_2 laser-foil interaction experiments observed the presence of sideband decay spectrum which was quite similar to ours. In conclusion, more theoretical work on parametric instabilities in strongly inhomogeneous plasmas are needed to get better agreement between experiment and theory.

ACKNOWLEDGEMENTS

*This work was supported by the Energy Research and Development Administration (formally the United States Atomic Energy Commission) contract E(11-1)-3073.

We thank Mr. J. Johnson and Mr. J. Taylor for their technical help.

REFERENCES

[1] NUCKOLLS, J. H., in Laser Interaction and Related Plasma Phenomena, Vol. 3B (Plenum Press, New York, New York, 1974) p. 399.

[2] PORKOLAB, M., in Symposium on Plasma Heating and Injection, (Editrice Compositori, Bologna, Italy, 1973) pp. 46,54; also in Symposium on Plasma Heating in Toroidal Devices, (Editrice Compositori, Bologna, Italy, 1974) pp. 28, 41.

[3] HARKER, K. J., and CRAWFORD, F. W., J. Geophys. Res. 75, 5459 (1970); PERKINS, F. W., and FLICK, J., Phys. Fluids 14, 2012 (1971); ROSENBLUTH, M. N., Phys. Rev. Lett. 29, 565 (1972); PESME, D., et al, Phys. Rev. Lett. 31, 203 (1973).

[4] DUBOIS, D. F., and GOLDMAN, M. V., Phys. Rev. Lett. 14, 544 (1965); NISHIKAWA, K. J., Phys. Soc. Japan 24, 916 (1968); ibid 24, 1152 (1968).

[5] PORKOLAB, M., Nuclear Fusion 12, 329 (1972).

[6] RIPIN, B., et al, Phys. Rev. Lett. 34, 1312 (1975).

[7] DREICER, H., ELLIS, R. F., and INGRAHAM, J. C., Phys. Rev. Lett. 31, 426 (1973).

[8] MIZUNO, K., and DEGROOT, J. S., University of California, Davis, Report R-4, 1975 (unpublished).

[9] EUBANK, H., Phys. Fluids 14, 2551 (1971).

[10] OKABAYASHI, M., CHEN, K., and PORKOLAB, M., Phys. Rev. Lett. 31, 1113 (L973).

[11] PORKOLAB, M., ARUNASALAM, V., LUHMANN, N. C., and SCHMITT, J., Paper E8 in the Fourth Annual Anomalous Absorption Conference, Lawrence Livermore Laboratory, April, 1974 (unpublished).

[12] PORKOLAB, M., ARUNASALAM, V., and LUHMANN, N. C., Plasma Physics 17, 405 (1975).

[13] THOMSON, J. J., FAEHL, R. J., KRUER, W. L., and BODNER, S., Phys. Fluids 17, 973 (1974).

[14] GREK, B., and PORKOLAB, M., Phys. Rev. Lett. 30, 836 (1973); also GREK, B., Ph.D. Thesis, Princeton University, 1975.

[15] NICHOLSON, D. W., and KAUFMAN, A. N., Phys. Rev. Lett. 33, 1207 (1974). SPATCHEK, K. H., SHUKLA, P. K., and YU, M. Y., Physics Letters 51A,183 (1975).

[16] WEINSTOCK, J., and BEZZERIDES, B., Phys. Fluids 16, 2287 (1973); also Phys. Rev. Lett. 32, 754 (1974).

[17] STAMPER, J. A., and RIPIN, B. H., Phys. Rev. Lett. 34, 138 (1975).

[18] GREK, B., Private communications; GREK, B., BALDIS, H., PEPIN, H., (to be published).

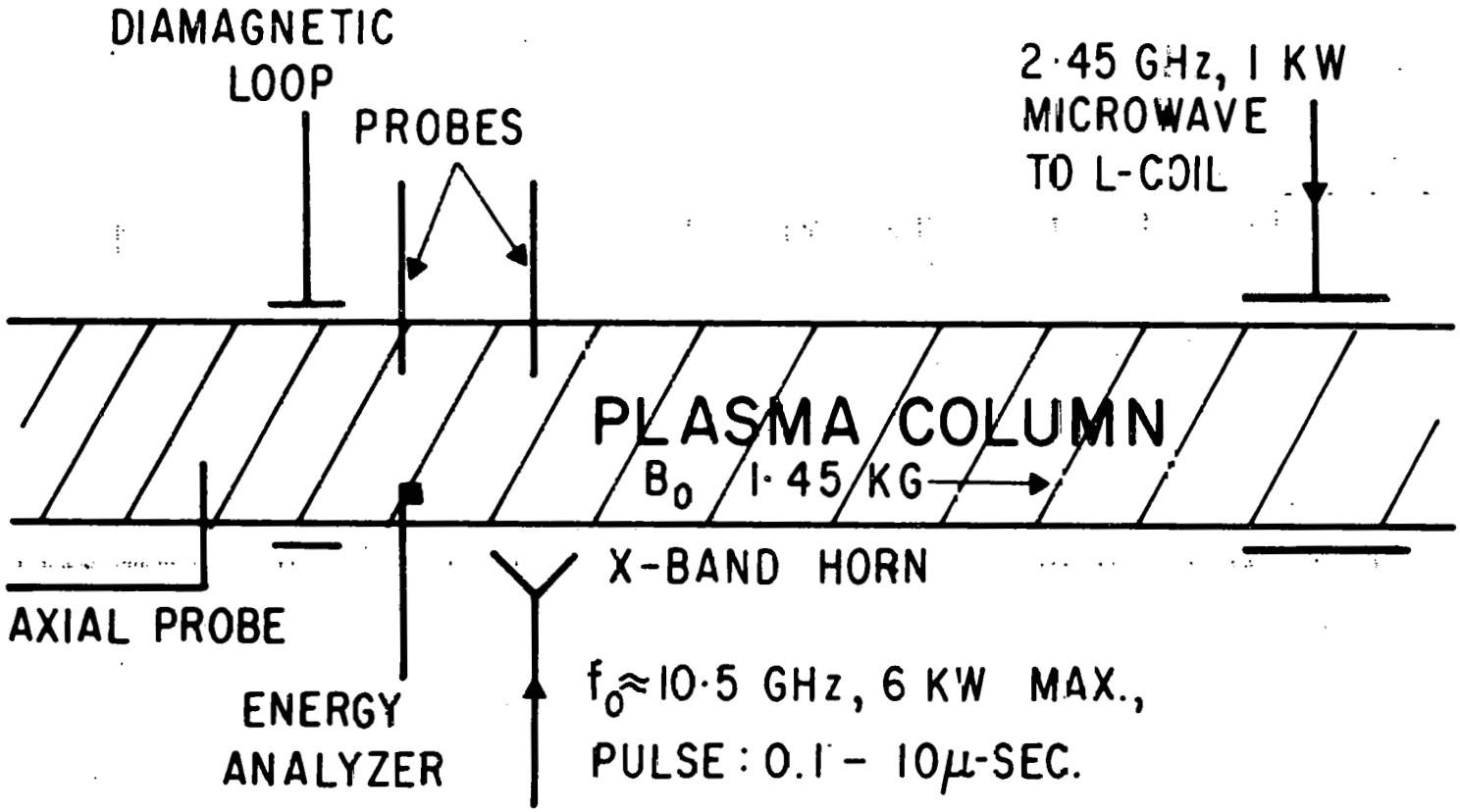

753524

Fig. 1. Experimental setup.

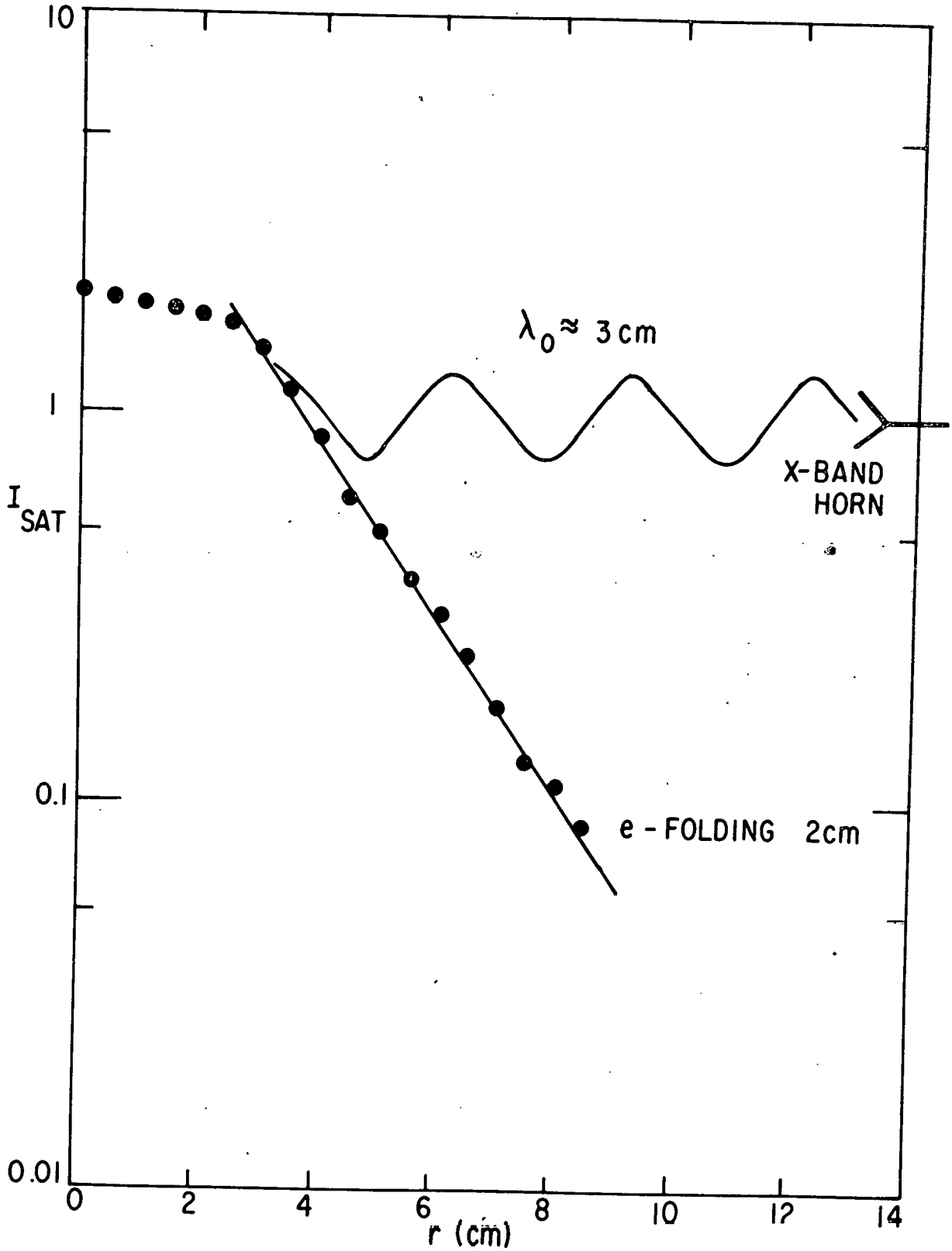

753528

Fig. 2. A typical density gradient (log scale) and a sketch of the free-space X-band wavelength.

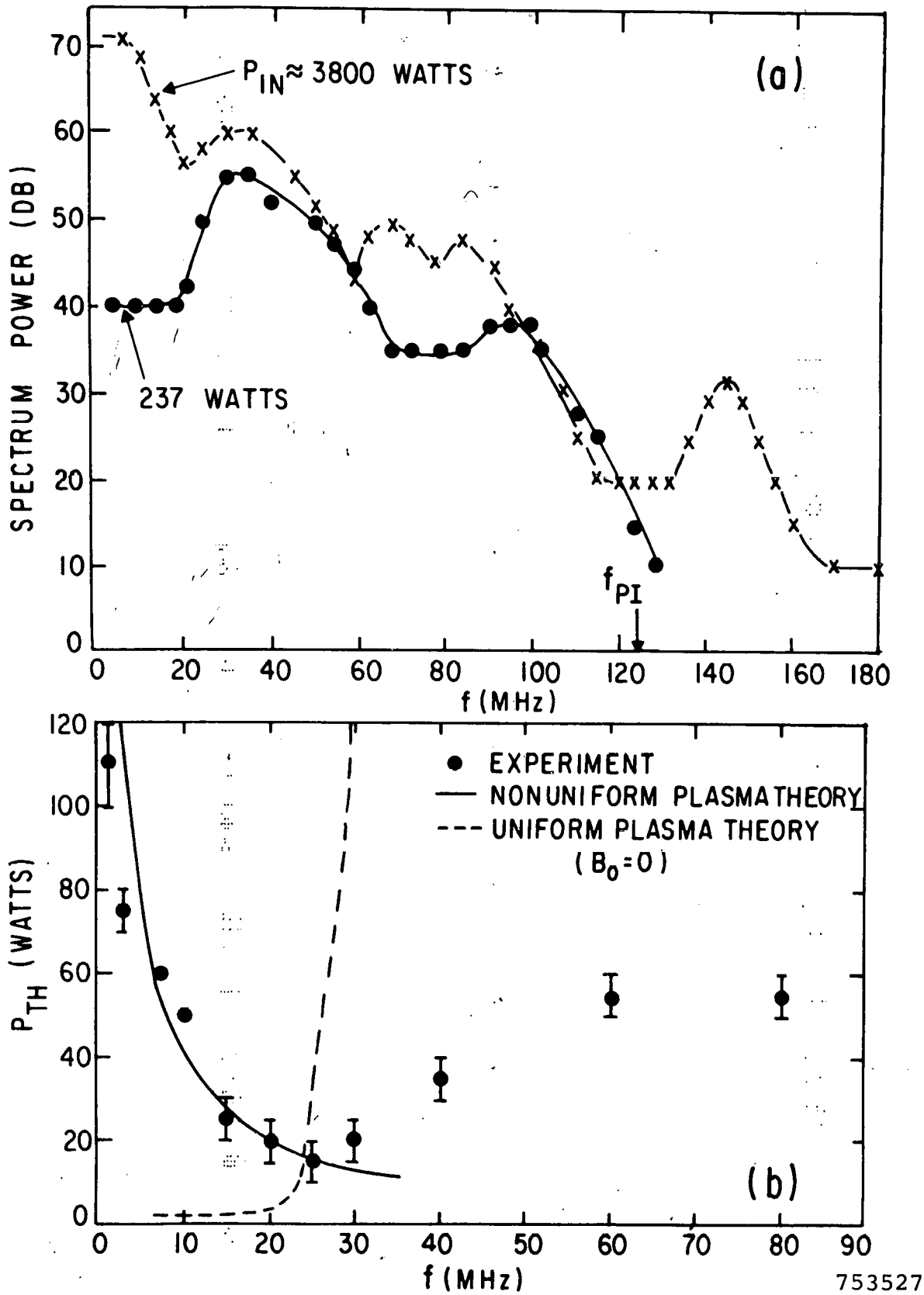

Fig. 3(a). Low frequency decay spectrum. O-mode.
Fig. 3(b). Experimentally measured thresholds at A = 1 (dots) uniform plasma theory (dashed line), and nonuniform plasma theory (solid line) (the latter calibrated on absolute scale from the incident power levels); O-mode.

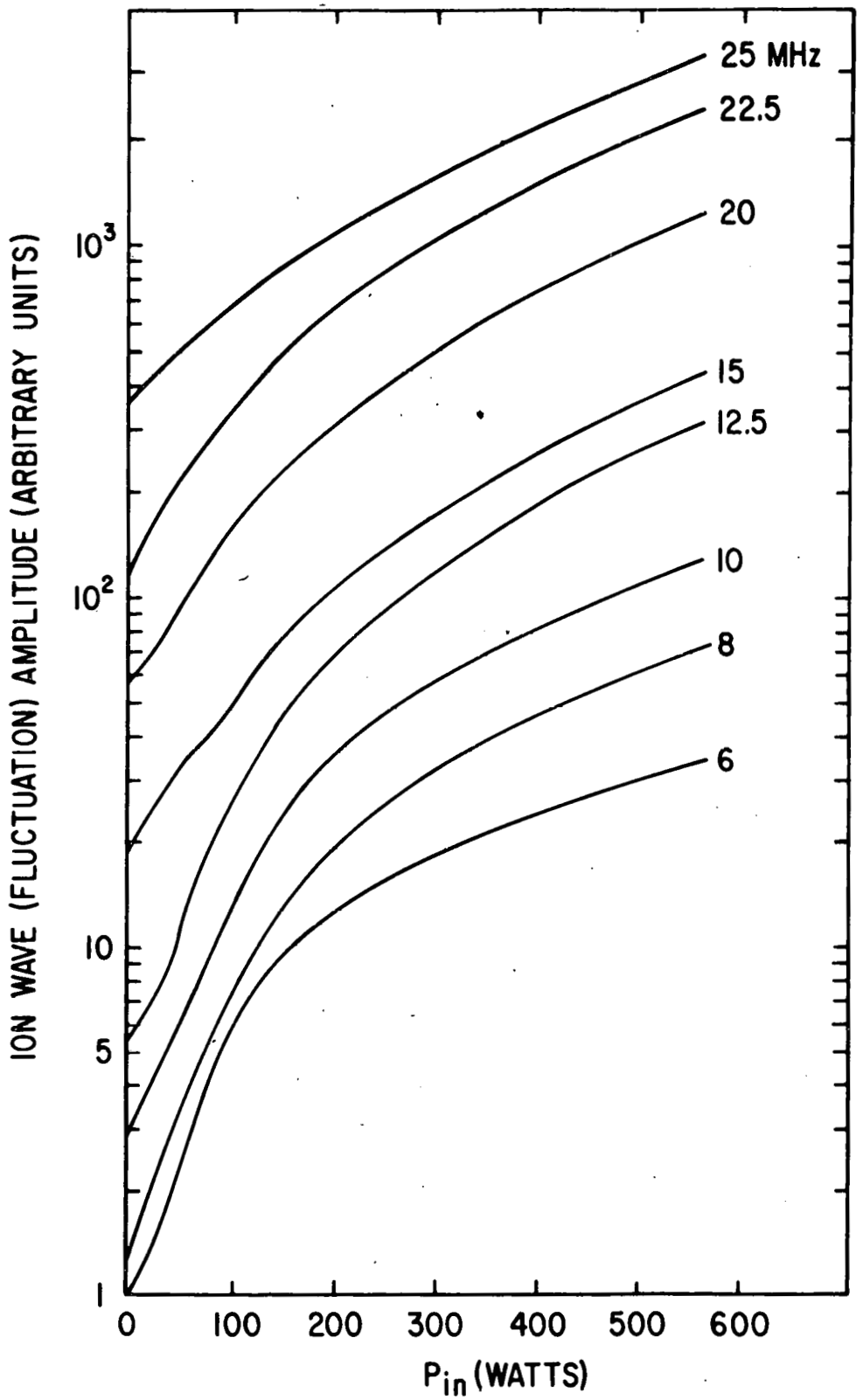

753530

Fig. 4. Amplification rates of background fluctuations for different frequencies. The density profile and the plasma diameter are different from that of Fig. (3); O-mode.

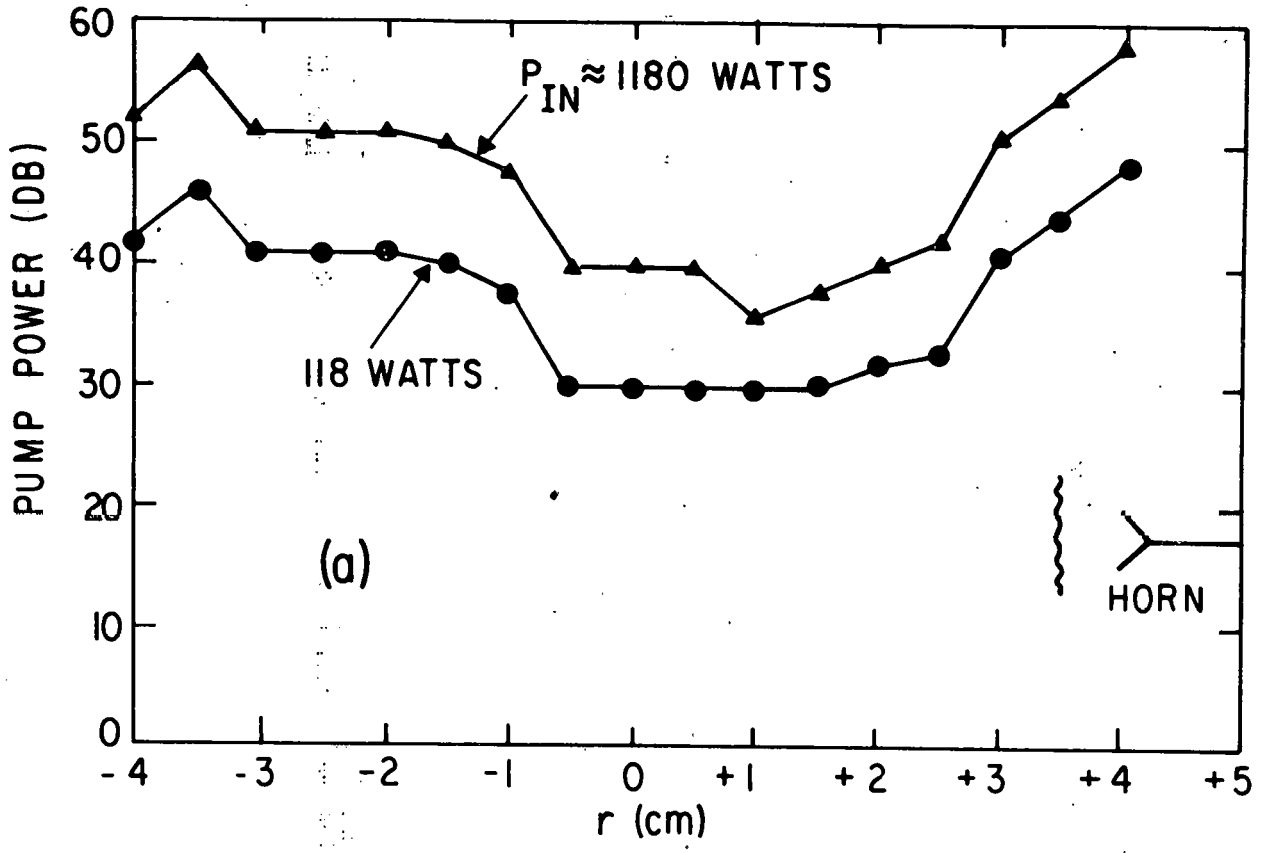

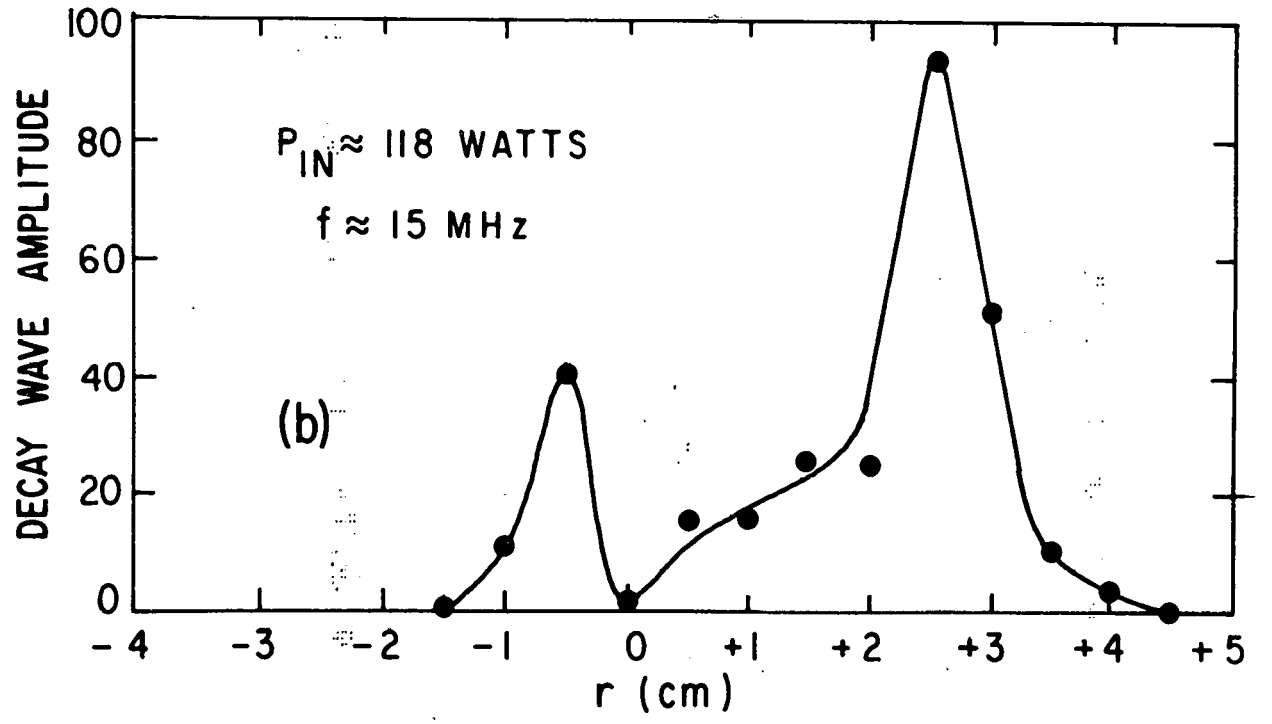

753529

Fig. 5(a). Relative pump power as a function of radius: O-mode.
Fig. 5(b). Localization of decay wave amplitude as a function of radius. P_{in} = 118 watts, f = 15 MHz; O-mode.

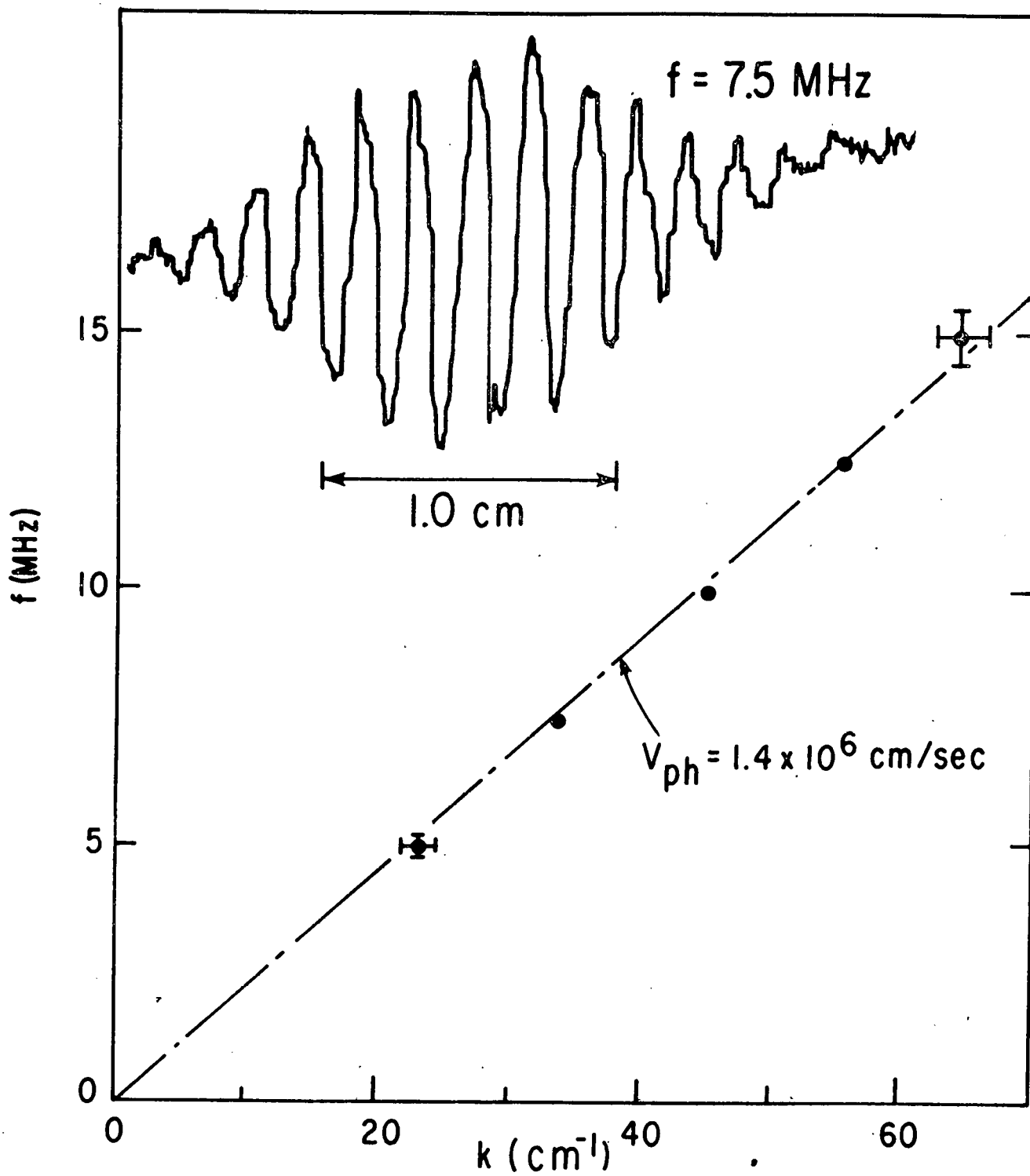

753525

Fig. 6. Ion acoustic wave dispersion relation obtained from parametrically pumped low frequency noise. Inset shows typical interferometer output about center of microwave horn near the critical layer; O-mode.

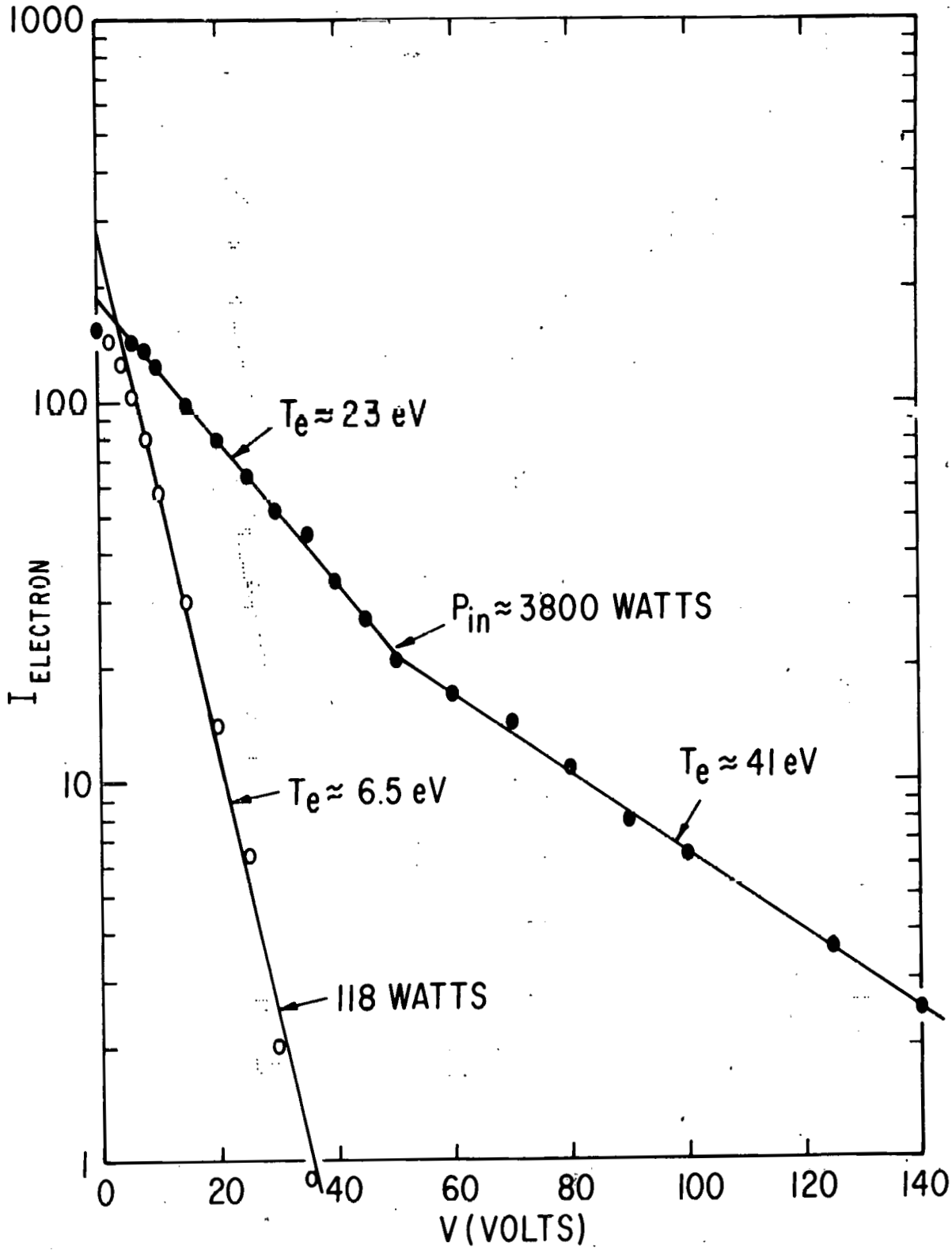

753522

Fig. 7. Energy analyzer measurements of the parallel electron energies; O-mode.

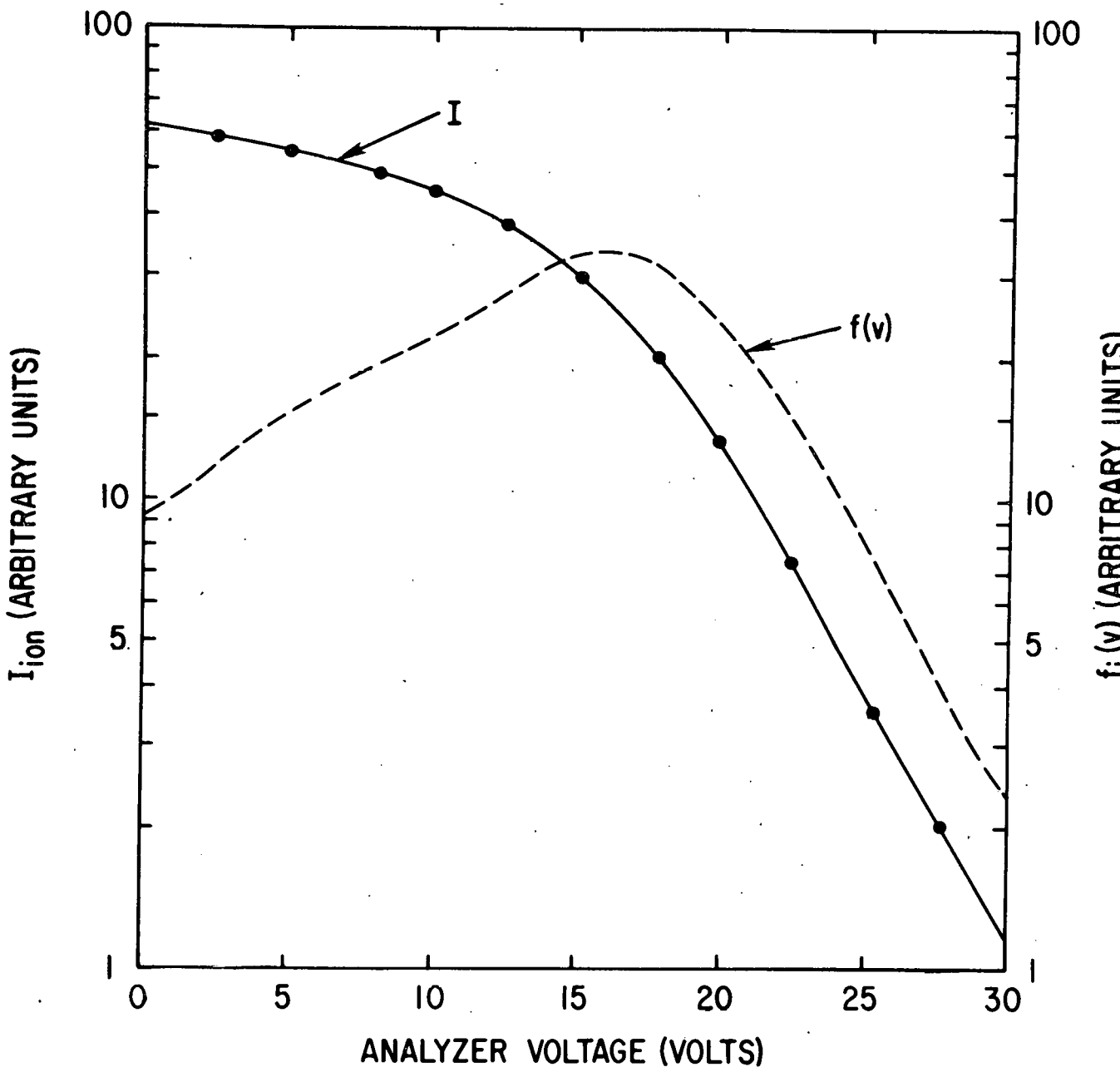

753531

Fig. 8. Energy analyzer measurements of the parallel ion energies (I), and distribution function deduced from these currents ($f_i(v)$); P_{in} = 3800 watts, τ = 10 μsec; O-mode.

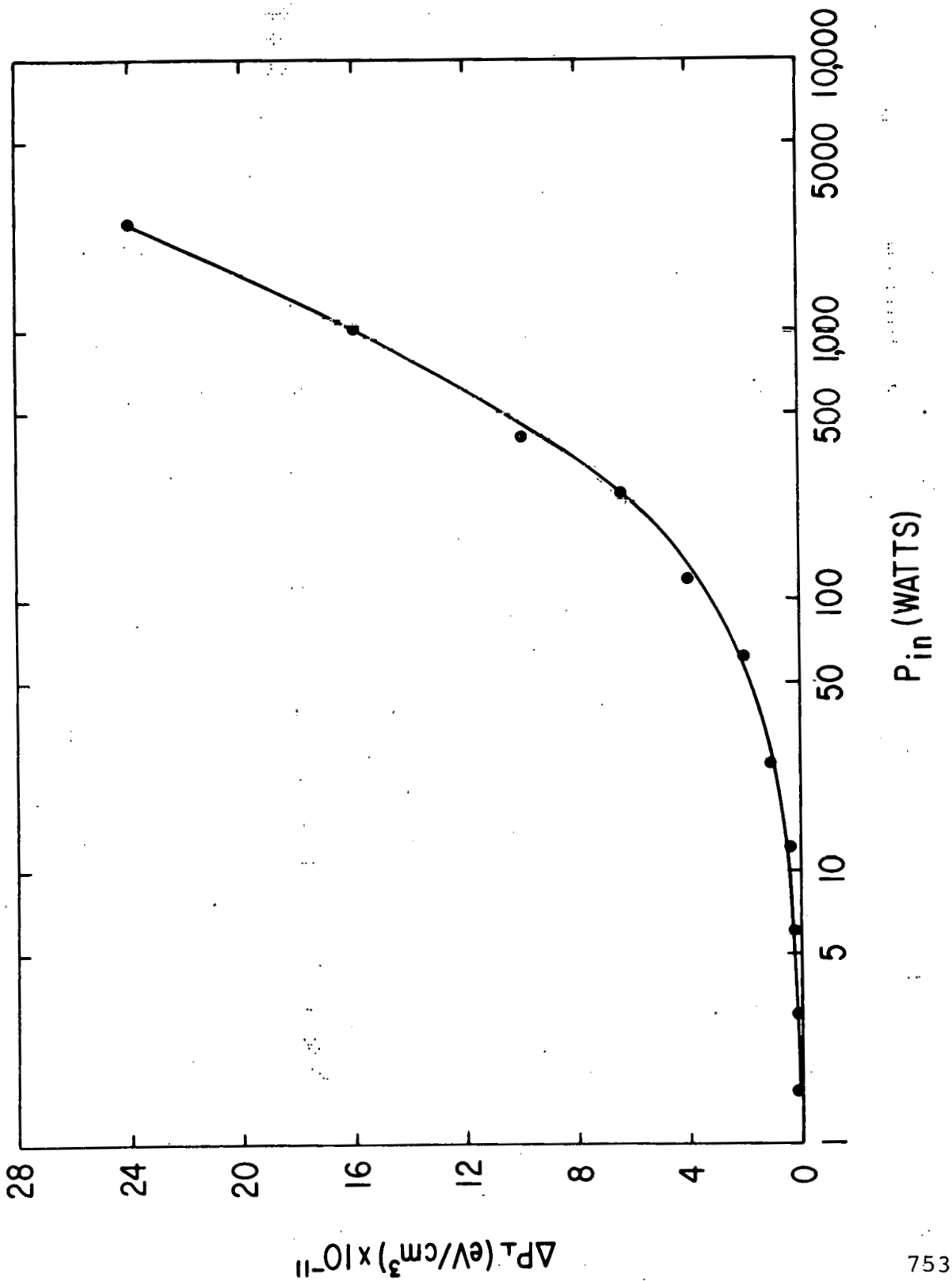

Fig. 9. Perpendicular energies as obtained by the shielded diamagnetic loop. Maximum perpendicular temperature change at P_{in} = 2500 watts give $\Delta T_\perp \simeq 2$ eV; O-mode.

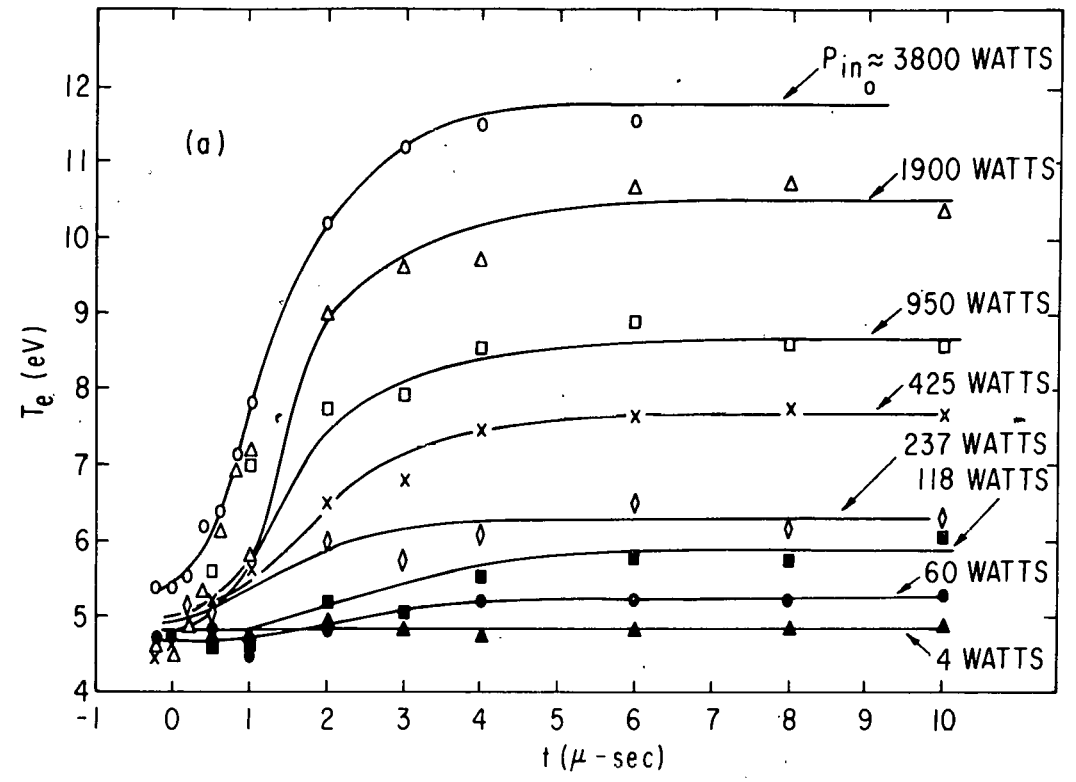

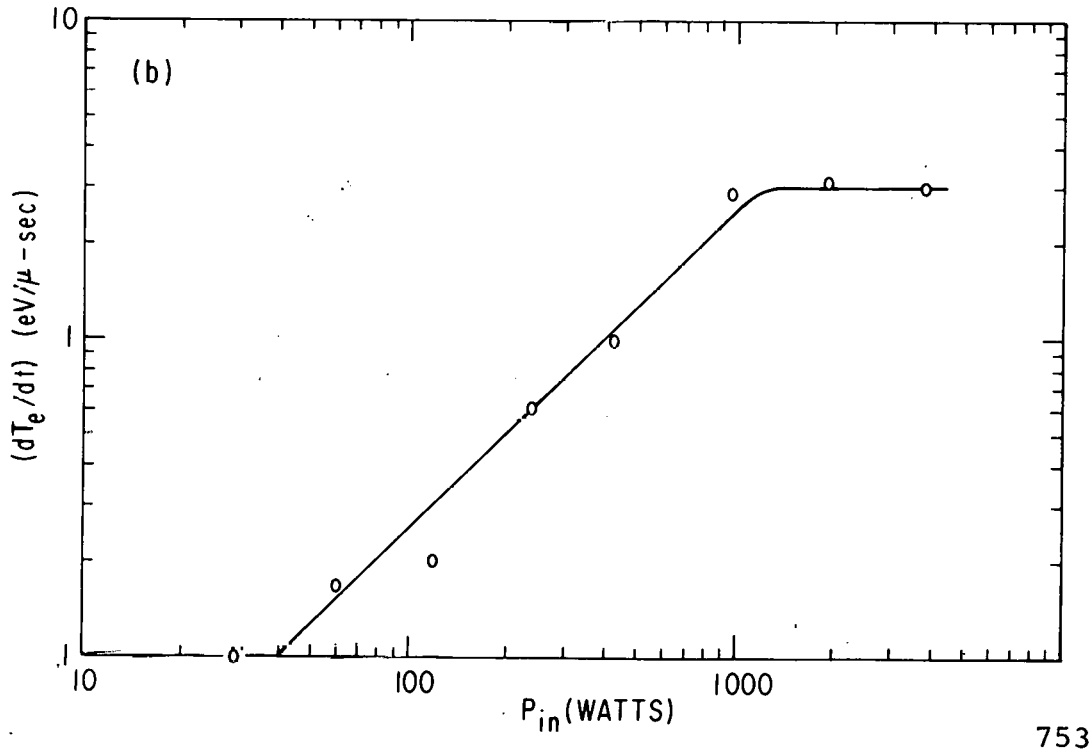

753535

Fig. 10(a). Temperature obtained from a Langmuir probe as a function of time and input power; O-mode.

Fig. 10(b). Initial heating rates in the first few micro-seconds as a function of power; O-mode.

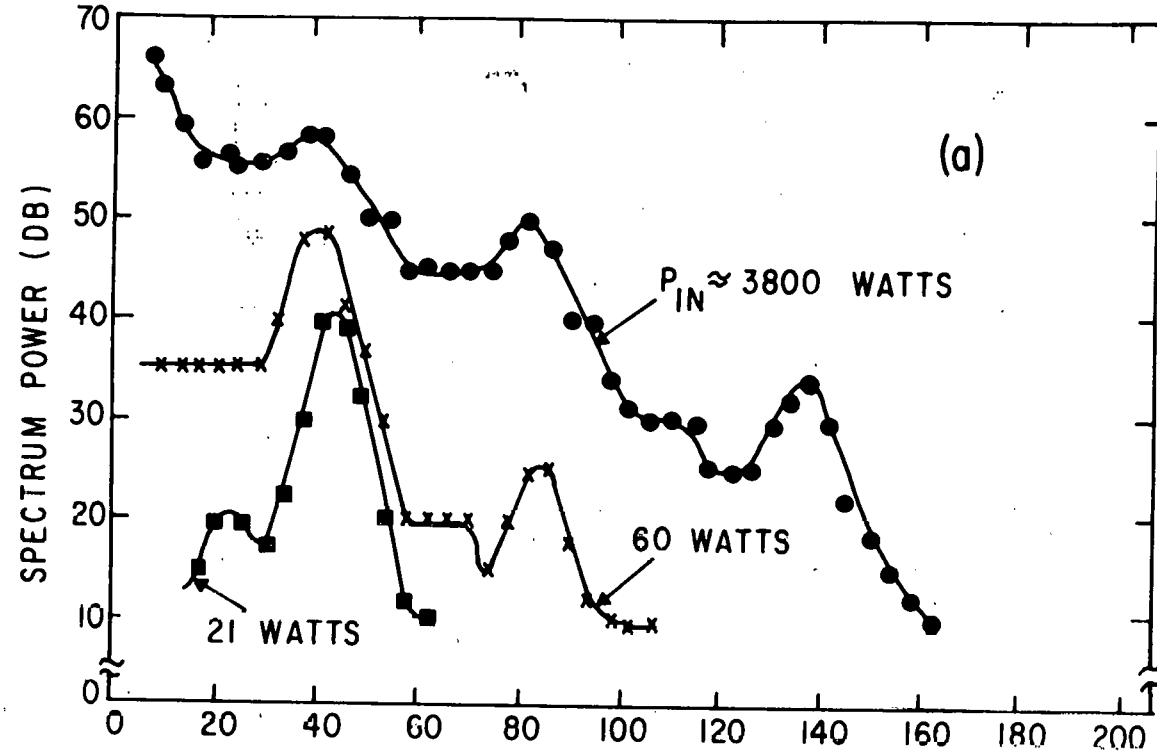

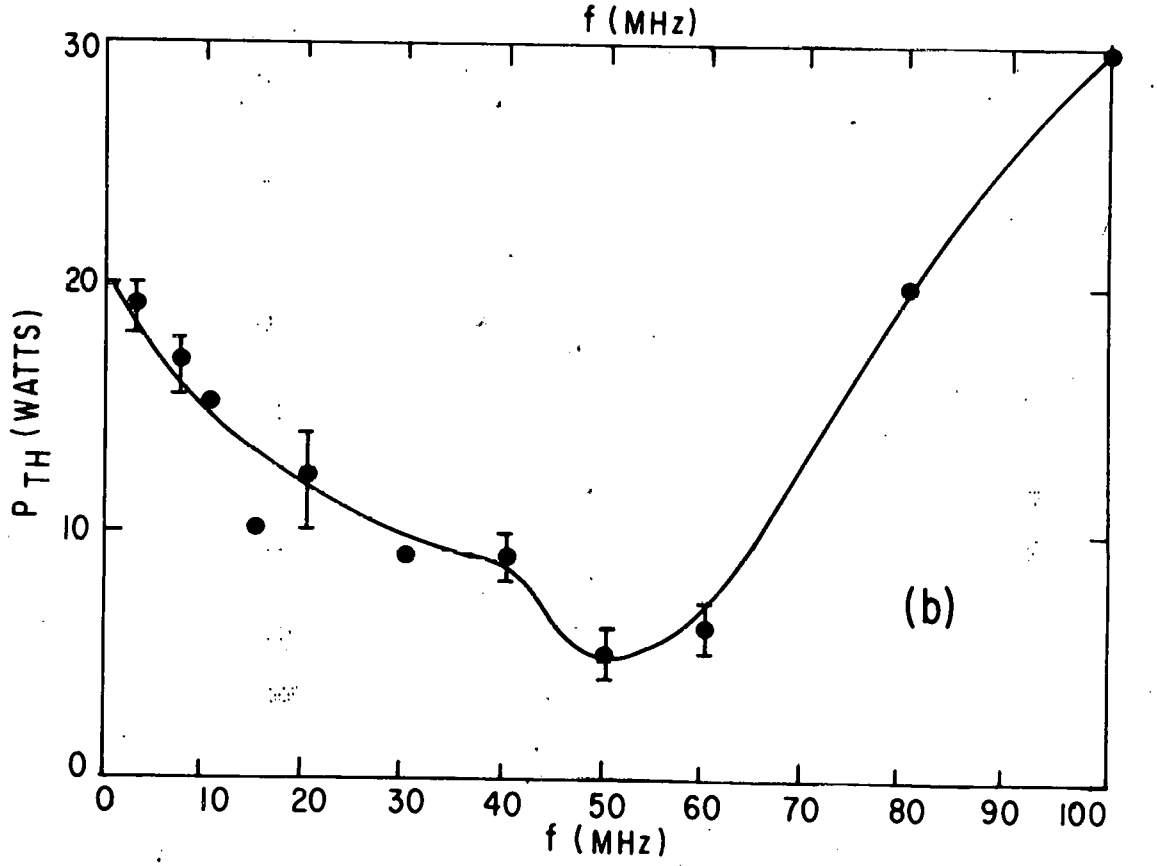

753526

Fig. 11(a). Decay spectrum in the EO mode at different input powers.

Fig. 11(b). Thresholds obtained in the EO mode, as a function of incident power.

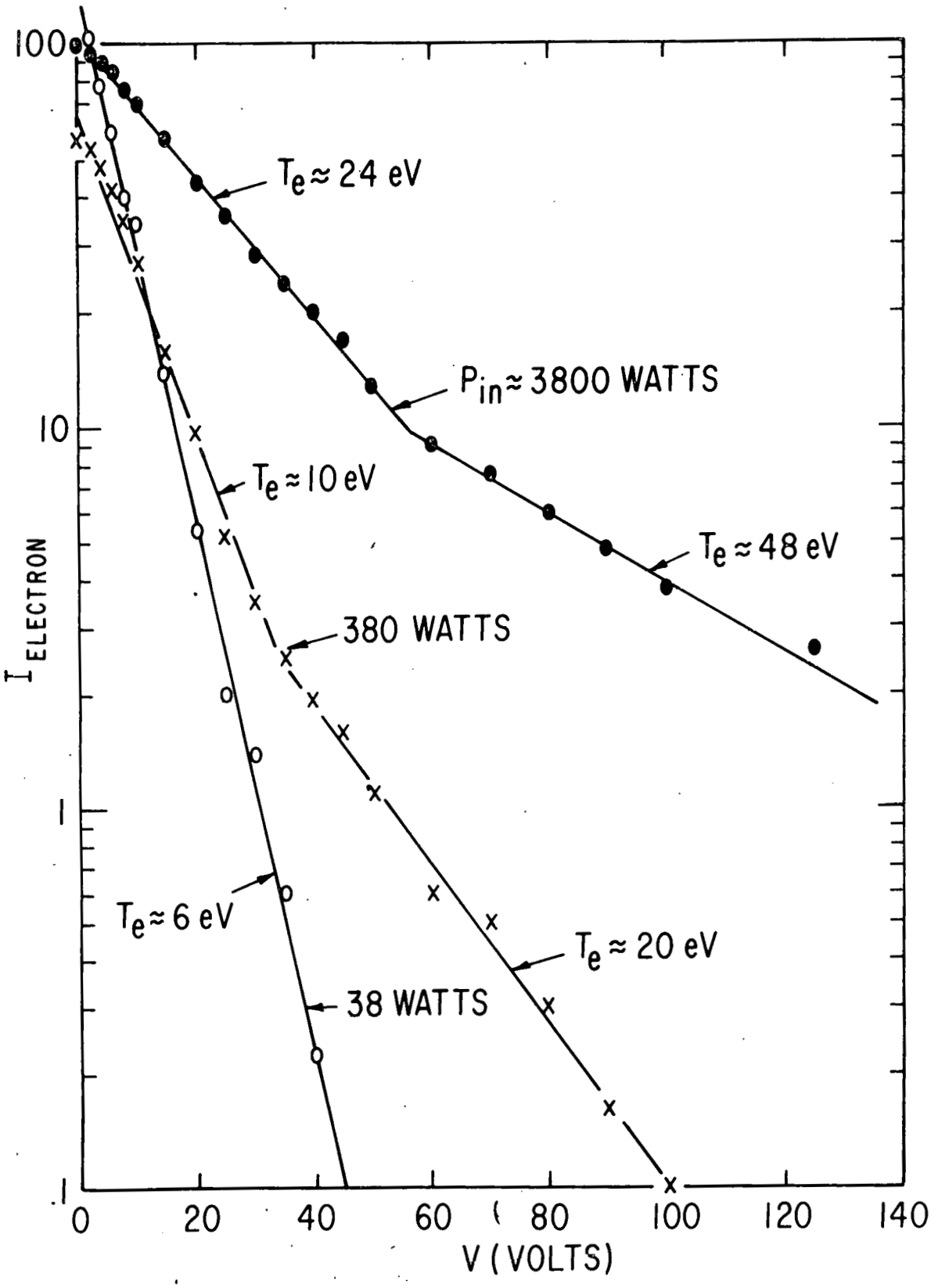

753523

Fig. 12. Energy analyzer measurements of the parallel electron energies. τ = 10 μsec; EO mode.

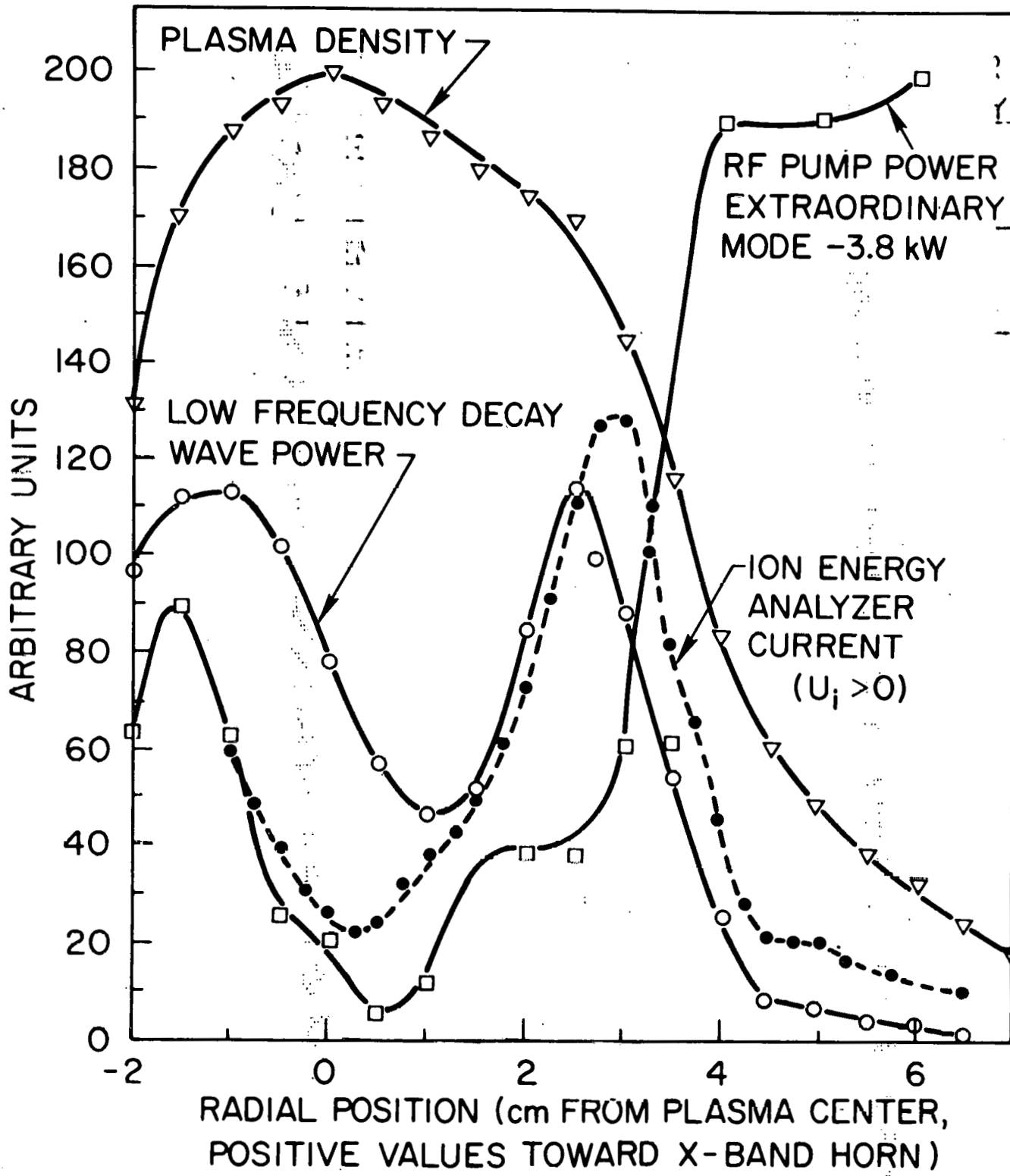

753533

Fig. 13. Localization of decay wave spectrum, ion energy, and relative RF pump power. P_{in} = 3800 watts.

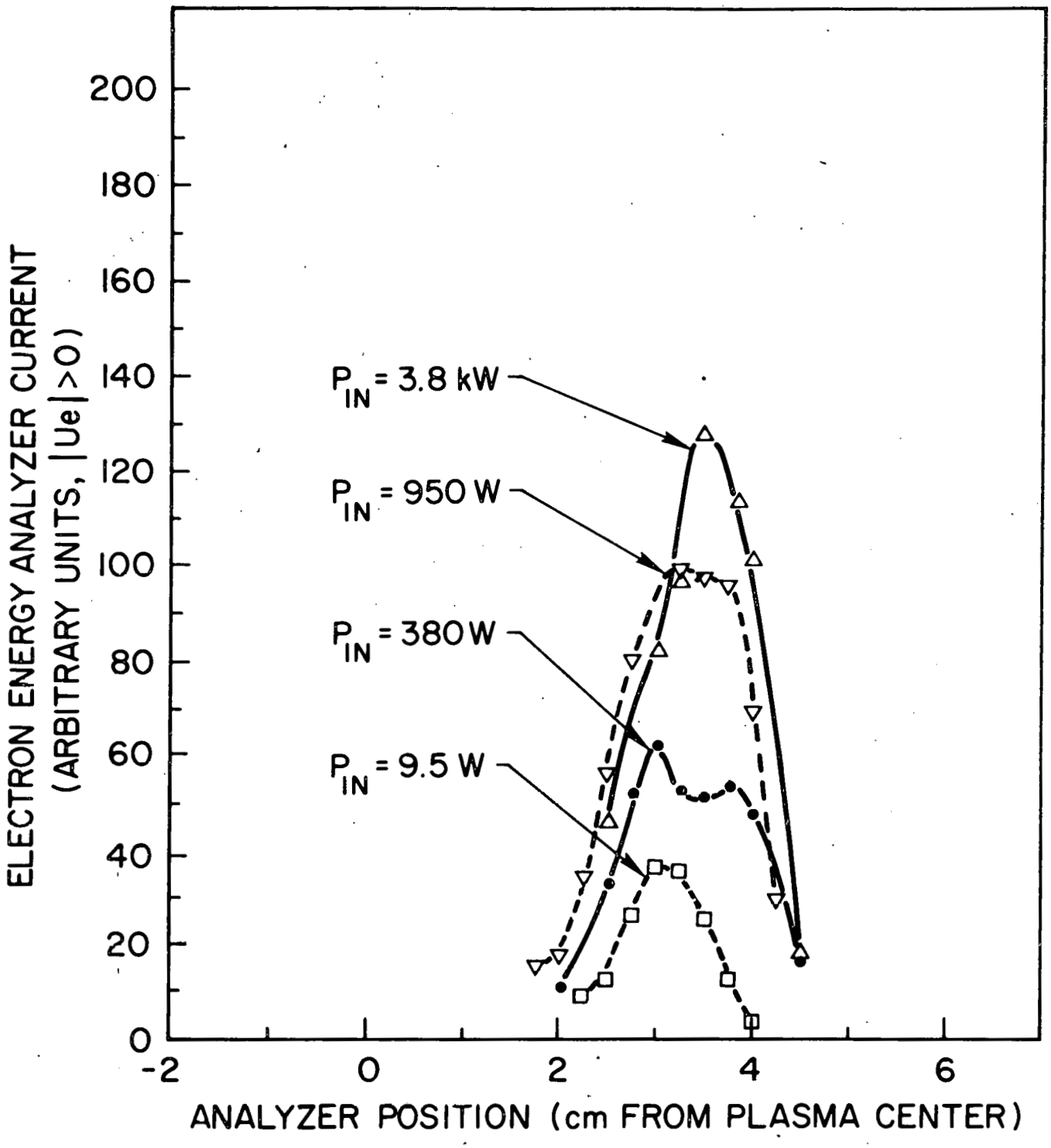

753532

Fig. 14. Localization of electron heating at different input powers under the conditions of Fig. 13.